

Minimalist Approach to 3-D Heart Modeling: A Novel Morphing Algorithm Relying on Four Anatomical Landmarks

MHD Jafar Mortada^{1,3}, Agnese Sbroolini¹, Laura Burattini^{1,*}, Peter Van Dam^{2,3}

¹Department of Information Engineering, Università Politecnica delle Marche, Ancona, Italy

²Center for Digital Medicine and Robotics, Jagiellonian University Medical Collage, Krakow, Poland

³Peacs BV, Nieuwerbrug, The Netherlands

Abstract

Computer heart modeling serves as a pivotal tool across diverse disciplines, facilitating the interpretation of electrical and mechanical information. The process of generating accurate patient-specific 3D heart model poses significant challenges, demanding time, expertise, and computational resources as established by both manual and artificial intelligent and deep-learning driven methods. In this paper, we introduce a novel morphing algorithm for generating 3D heart models with minimal input. By pinpointing four key anatomical landmarks which are the heart apex and the centers of the Mitral, Pulmonary, and Tricuspid valves - our approach leverages a template model for the ventricles. This algorithm scales the ventricles of the heart along their primary axes and aligns them using translation and rotation based on the landmark locations. It was tested on a dataset of 94 models revealing promising outcomes, both visually and quantitatively. Specifically, the median percentage error in the estimation of endocardial left volume and of endocardial right volume are lower than 13% and 6%, respectively. Importantly, our method offers a rapid, efficient alternative, making it accessible to a broader range of users which would open the way for a new modeling method that is fast and might satisfy the need in inverse ECG applications.

1. Introduction

The demand for cardiac 3-D models has recently risen due to their ability to integrate both electrical and mechanical info on the heart[1]. Moreover, 3-D models are needed to solve the inverse problem of electrocardiography [2], which consists in reconstructing cardiac electrical activity from body surface electrocardiographic (ECG) measurements.

In the literature, many algorithms proposed generic models, called template models, by combining multi-subject models [3]. The main issue related to these

template models is the lack of subject-specific anatomy, that should be preserved to guarantee the clinical evaluation.

To create subject-specific models, 3-D cardiac images of the subject (acquired by computed tomography and/or magnetic resonance imaging) must be acquired and processed to perform semantic segmentation. Such operation may be a cumbersome task[4] using manual methods. Indeed, this procedure is time consuming, it requires very strong clinical experience, and it is influenced by subjectivity. Recently, deep learning approaches proposed solutions in the field of semantic segmentation [5], but this procedure is resource-demanding due to the big size of the images, the multiple structures to be segmented, and the complex structure of the deep learning architecture [6].

Cardiac landmarks can be detected manually or even by using deep-learning approaches with less complicated models used for fully cardiac semantic segmentation. In Figure 1, the heart apex (HA), the mitral valve center (MVC), the pulmonary valve center (PVC) and the tricuspid valve center (TVC) landmarks are shown.

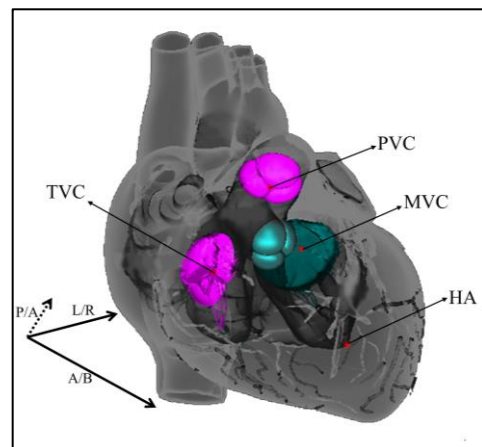


Figure 1. Representation of the identification of the four cardiac anatomical landmarks, and the cardiac axis, Posterior/Anterior (P/A), Left/Right (L/R), and Apex/Base (A/B).

By considering the template models in the literature [3], the perfect modelling algorithm should compute only the four cardiac anatomical landmarks from the 3-D images and use them to morph a template model, obtaining a subject-specific model. Thus, the aim of this study is to propose a morphing algorithm for 3-D subject-specific model construction by using a template model [3] and only four cardiac anatomical landmarks.

2. Material and Methods

2.1. Data

Data includes 94 computerized tomography images acquired from 94 subjects (50 males and 43 females) [7-9]. For each 3-D image, the four anatomical landmarks were extracted, and patient-specific model of the ventricles was constructed by experts' manual segmentation [10] Thus, the included structures are the epicardium, the left and the right ventricle endocardium, mitral valve ring, tricuspid valve ring, and pulmonary valve ring. The models were triangulated, preserving their spatial orientation within the chest cavity. These models were used as ground truth of the morphing algorithm.

The considered single template model is the one used in previous study [11], The four cardiac anatomical landmarks of the template model are calculated, that are Heart apex ($\bar{H}A$), Mitral valve center ($\bar{M}VC$), Pulmonary Valve center ($\bar{P}VC$) and Tricubes valve center($\bar{T}VC$).

2.2. Morphing Algorithm

The morphing algorithm (Figure 2) considers as inputs four anatomical heart landmarks of the subject: $\bar{H}A$, $\bar{M}VC$, $\bar{P}VC$ and $\bar{T}VC$.. The morphing procedure consists of two steps: scaling and alignment. Scaling is performed by using a scaling factor along the cardiac apex-base axis (A/B, Figure 1), the cardiac left-right axis (L/R, Figure 1) and the cardiac posterior-anterior axis (P/A, Figure 1). The ratio between $\bar{H}A$ - $\bar{M}VC$ and $\bar{H}A$ - $\bar{M}VC$ distances is used as A/B factor.

The ratio between $\bar{M}VC$ - $\bar{T}VC$ and $\bar{M}VC$ - $\bar{T}VC$ distances is used as L/R factor. Finally, the valve planes of the subject and of the template model are established by using $\bar{H}A$, $\bar{M}VC$, and $\bar{T}VC$ and $\bar{H}A$, $\bar{M}VC$, and $\bar{T}VC$, respectively; then, $\bar{P}VC$ and $\bar{P}VC$ are projected into planes. The ratio of the distance between $\bar{P}VC$ and its projection and the distance between $\bar{P}VC$ and its projection is used as P/A factor. Alignment is done by translating the scaled template until the $\bar{H}A$ and $\bar{H}A$ are aligned ($\bar{H}A = \bar{H}A$). Then, the angle between $\bar{H}A$ - $\bar{M}VC$ vector and $\bar{H}A$ - $\bar{M}VC$ vector is computed, and the scaled/translated model is rotated accordingly using $\bar{H}A$ as center of rotation ($\bar{H}A$ - $\bar{M}VC$ vector = $\bar{H}A$ - $\bar{M}VC$ vector). Finally, the projections of $\bar{P}VC$ and $\bar{P}VC$ on the plane defined by $\bar{H}A$ and $\bar{H}A$ - $\bar{M}VC$ vector are computed. The angle between these projections is computed, and the scaled/translated/rotated model is rotated accordingly using $\bar{H}A$ - $\bar{M}VC$ vector as rotation axis, becoming the morphed model.

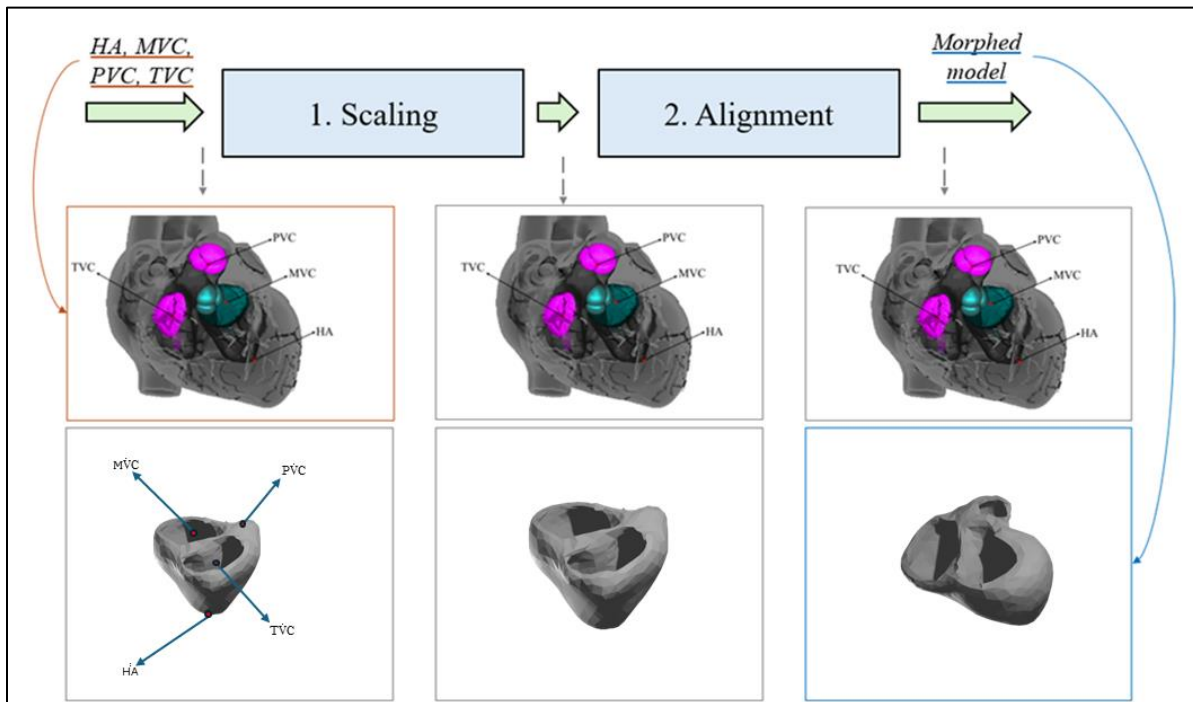


Figure 2. Block diagram and a representative example of the morphing algorithm.

2.3. Statistics

In order to evaluate the goodness of fit produced by the morphing algorithm, anatomical features were computed between the ground truth models and on the morphed models: a) endocardial left volume (LV, mm³), b) the endocardial right volume (RV, mm³), c) the angle between the plane of the mitral valve and the anatomical y-axis (α_{MV} , °), d) the angle between the plane of the pulmonary valve and the y-axis (α_{PV} , °), e) the angle between the plane of the tricuspid valve and the y-axis (α_{TV} , °), and f) the angle between the plane of the heart base and the y-axis (α_{HB} , °). Normality of the distributions of anatomical features are evaluated by the Lilliefors test and non-normal distributions are reported in terms of 50th[25th;75th] percentiles. Error (ϵ) and percental error ($\% \epsilon$) are computed.

Moreover, geometrical distances are computed between anatomical reference points of the ground truth models and of the morphed models. They are the distance between the MVC (Δ_{MVC} , mm), the distance between the PVC (Δ_{PVC} , mm), and the distance between the TVC (Δ_{TVC} , mm). The minimal distances between the points of the endocardial left volumes (δLV , mm), the minimal projected distances between the points of the endocardial right volumes (δRV , mm), and minimal distances between the points of the valve planes (δVP , mm). For each subject, the average ($\mu_{\delta LV}$, $\mu_{\delta RV}$, $\mu_{\delta VP}$) and the standard deviation ($\sigma_{\delta LV}$, $\sigma_{\delta RV}$, $\sigma_{\delta VP}$) of δLV , δRV , and δVP are extracted. Normality of the distributions of geometrical distances is evaluated by the Lilliefors test and non-normal distributions are reported in terms of 50th[25th;75th] percentiles.

3. Results

Figure 3 shows an example of the results: the morphed model (depicted in yellow) is superimposed with the ground truth model (depicted in red), obtained from the clinical manual segmentation.



Figure 3. Graphical example of an obtained morphed

model (in yellow) and its ground truth model (in red).

Distributions of the anatomical features and geometrical distances are reported in Table 1 and Table 2, respectively. Overall, the performance of the morphing algorithms is very good with the median relative error lower than 13% for LV and 6% for RV; the valve distance is good, with median values lower or equal to 17mm. Finally, the minimal distance between the endocardial left volume, the endocardial right volume, and the valve plane present median values lower than 2 mm, associated with a median standard deviation lower than 9 mm.

Table 1. Distributions of the anatomical features, also including the errors and the relative errors.

	Ground Truth	Morphed Models	ϵ	rel ϵ [%]
LV (mm ³)	148 [109;178]	126 [103;145]	18 [-1;44]	13 [-1;27]
RV (mm ³)	132 [110;167]	124 [100;142]	8 [-11;36]	6 [-9;21]
α_{MV} (°)	42 [38;49]	43 [39;49]	-2 [-3;1]	-3 [-9;1]
α_{PV} (°)	76 [66;83]	68 [62;74]	17 [13;26]	9 [0;17]
α_{TV} (°)	42 [32;48]	48 [43;54]	-6 [-13;-1]	-14 [-34;-2]
α_{HB} (°)	43 [37;50]	47 [42;52]	-3 [-7;0]	-7 [-16;0]

Table 2. Distributions of the geometrical distances.

	Distribution
Δ_{MVC} (mm)	12 [8;15]
Δ_{PVC} (mm)	17 [12;22]
Δ_{TVC} (mm)	17 [13;25]
$\mu_{\delta LV}$ (mm)	-2 [-4;-1]
$\sigma_{\delta LV}$ (mm)	4 [4;5]
$\mu_{\delta RV}$ (mm)	-2 [-4;0]
$\sigma_{\delta RV}$ (mm)	6 [5;7]
$\mu_{\delta VP}$ (mm)	0 [-2;1]
$\sigma_{\delta VP}$ (mm)	9 [7;11]

4. Discussion

The presented study proposed a novel and simple morphing algorithm for 3-D subject-specific model construction by using a template model and only four cardiac anatomical landmarks. The main novelty of the method is connected to the use of the four anatomical landmarks, that can be extracted from 3-D cardiac imaging techniques. The method requires only the coordinates of the landmarks, that can be derived from cardiac imaging. Finally, the computational efforts of this morphing algorithm are very low, because it is not associated with the high level of computational complexity, typical of image processing techniques. For the moment, the algorithm is able to morph only the ventricular chambers, without considering the geometry of the atria. Future studies will investigate the inclusion of atrial anatomy, in order to be able to morph the entire heart.

To evaluate the ability of the morphing algorithm, its performance was compared with the manual segmentation performed by experts. The initial results are good, and the extracted features show promising results in terms of capturing the basic characteristics of the ventricles.

Of note, this version of the morphing algorithm considers an existing 3-D template, the one presented in the literature. Thus, having general multiple cardiac 3-D template is desirable, guaranteeing the possibility to match the best template with the heart of the subject of interest. Thus, future studies will evaluate the quality of the used 3-D models and, eventually, will define novel 3-D model classes that can be used to morph hearts of patients with specific diseases.

In the literature, the main used algorithms for 3-D cardiac modeling are based on deep-learning semantic segmentation [5]. Unfortunately, the used dataset does not include annotated images that can be used to perform a quantitative comparison with our morphing algorithm. By considering the qualitative characteristics of these deep-learning algorithms, they require a huge number of data to be trained and validated; they present a high computational complexity, considering as input 3-D cardiac images, and they are not scalable because, due to their data dependency, a different deep-learning model has to be trained for each type of imaging technique. Thus, considering its interpretability and scalability, our novel morphing algorithm seems to be a good solution for the construction of cardiac 3-D models.

4. Conclusion

The novel morphing algorithm is able to efficiently morph the cardiac ventricles, providing a reliable subject-specific 3-D model. Future studies will integrate the morphed cardiac atria and the use of multiple 3-D model templates.

References

- [1] S. M. Szilágyi, L. Szilágyi, and Z. Benyó, "A Patient Specific Electro-Mechanical Model of the Heart," *Comput Methods Programs Biomed*, vol. 101, no. 2, pp. 183–200, Feb. 2011.
- [2] A. Kalinin, D. Potyagaylo, and V. Kalinin, "Solving the Inverse Problem of Electrocardiography on the Endocardium Using a Single Layer Source," *Front Physiol*, vol. 10, no. FEB, 2019.
- [3] C. Mauger et al., "Right Ventricular Shape and Function: Cardiovascular Magnetic Resonance Reference Morphology and Biventricular Risk Factor Morphometrics in UK Biobank," *Journal of Cardiovascular Magnetic Resonance*, vol. 21, no. 1, Jul. 2019.
- [4] X. Zhuang, "Challenges and Methodologies of Fully Automatic Whole Heart Segmentation: A Review," *J. Healthc. Eng.*, vol. 4, pp. 371-408, Mar. 2013.
- [5] C. Chen et al., "Deep Learning for Cardiac Image Segmentation: A Review," *Frontiers Media S.A.*, vol. 7., Mar. 2020.
- [6] S. Park and M. Chung, "Cardiac Segmentation on CT Images Through Shape-Aware Contour Attentions," *Comput Biol Med*, vol. 147, p. 105782, Aug. 2022.
- [7] Roudijk R.W. et al., "Comparing Non-Invasive Inverse Electrocardiography with Invasive Endocardial and Epicardial Electroanatomical Mapping During Sinus Rhythm," *Front. Physiol.*, vol. 12, Oct. 2021.
- [8] Asatryan B. et al., "Man vs Machine: Performance of Manual vs Automated Electrocardiogram Analysis for Predicting the Chamber of Origin of Idiopathic Ventricular Arrhythmia," *J Cardiovasc Electrophysiol.*, vol. 31, no. 2, pp. 410-416, Dec. 2020.
- [9] Sedova K.A., van Dam P.M., Blahova M., Necasova L., and Kautzner J., "Localization of the Ventricular Pacing Site from BSPM and Standard 12-Lead ECG: A Comparison Study," *Sci. Rep.*, vol. 13, no. 1, Jun. 2023.
- [10] van Dam P.M., Gordon J.P., Laks M.M., and Boyle N.G., "Development of New Anatomy Reconstruction Software to Localize Cardiac Isochrones to the Cardiac Surface from the 12-Lead ECG," *J Electrocardiol.*, vol. 48, no. 6, pp. 959–965, Nov. 2015.
- [11] M. J. Boonstra, D. H. Brooks, P. Loh, and P. M. van Dam, "CineECG: A Novel Method to Image the Average Activation Sequence in the Heart from the 12-Lead ECG," *Comput Biol Med*, vol. 141, p. 105128, Feb. 2022.

Address for correspondence:

Laura Burattini.
Università Politecnica delle Marche,
Department of Information Engineering,
Via Breccia Bianche, 60131 Ancona, Italy.
E-mail address. l.burattini@univpm.it.